Identification of an Unknown Radioactive Source using Gamma Ray Spectroscopy

Kellie McGuire[1,*] and Ronny Nguyen[1]

[1] *Department of Physics, University of New Hampshire*

(Dated: October 3, 2018)

We identified an unknown radioactive source by measuring its gamma emission spectrum using a NaI scintillator with photomultiplier. To calibrate the experiment we measured the spectra of two known radioactive sources and mapped their energy photopeaks to the channels of a multichannel analyzer. This enabled us to identify the unknown source as Bismuth-207. We used this same experimental setup to measure the mass attenuation coefficient of lead at 609 keV, the results of which are consistent with published values.

INTRODUCTION

Human beings are constantly exposed to background radiation. Most of this radiation occurs naturally, in the form of cosmic rays and from minerals and gases in the Earth's crust [1]. Exposure to some amount of background radiation is inevitable, and when limited in dose, this radiation does not pose a measurable risk to living organisms [2]. However, certain environmental factors, both natural and artificial, can increase exposure to background radiation beyond safe levels. For instance, some ore mines can exhibit abnormally high levels of background radiation [3], as can regions heavily influenced by nuclear accidents [4]. Because exposure to high levels of ionizing radiation poses a health risk to living organisms, the ability to detect and identify radioactive sources is crucial in assessing the safety of these regions.

In this experiment, we demonstrate a method for identifying a radioactive material by measuring its gamma ray emissions using a NaI scintillator. We also show how this same method can be used to measure the effectiveness of lead at absorbing gamma ray energy, the results of which could prove useful in the development of radiation shielding.

BACKGROUND

Decay of radioactive materials.—Radioactive elements are unstable nuclei that spontaneously decay to lower-energy states, emitting their excess energy as radiation. The rate of this decay is governed by quantum mechanics and is probabilistic. The lifetime of a radioactive sample is characterized by its half-life: the time necessary for a collection of identical radionuclides to reduce to half their initial number. Given a large enough sample, one can observe this decay directly in the lab.

In general, a radioactive nucleus can undergo many different decays before reaching its final, stable state [5]. These decays are governed by conservation laws, such that only certain decay schemes can occur for a given radionuclide [6]. Further, each possible decay occurs with a definite probability. Radioactive materials can thus be identified by the products of their decay, which act as the signature of the radioactive sample.

Scintillator method.—Scintillating materials are commonly used as radioactivity detectors because they emit visible light when struck by charged particles. This light can either be observed directly or translated into energy information, as is done in this experiment.

In the case of gamma ray detection, the incident photon must transfer its energy to a charged particle (electron) before it can be detected by the scintillator. This occurs via three main mechanisms: the photoelectric effect, Compton scattering, and pair production [7]. Whereas in the photoelectric effect and pair production the gamma ray is completely absorbed, in Compton scattering the photon deposits only part of its energy. The recoiling photon is then left to either interact with another electron or escape the detector altogether. As a result, energy resolution is lost in the region where Compton scattering is dominant. A NaI detector is well-suited for gamma ray spectroscopy because its photoelectric and pair production cross-sections are much larger than its Compton scattering cross-section [7].

EXPERIMENTAL SETUP

A NaI crystal was used to detect gamma rays emitted by the radioactive samples (Fig. 1). The NaI crystal was coupled to a photomultiplier (Bicron 2M2/2), which amplified the resulting photoelectric current through a series of high-voltage dynodes. The amplified current was then converted to a voltage and directed through a spectroscopic amplifier (Ortec 672).

The signal was observed on an oscilloscope, and the amplification was increased until it fell just below saturation. This signal was then directed to a multichannel analyzer (Ortec Easy-MCA), which sorted each pulse (decay event) into a channel according to its amplitude (energy). The emission spectra were then observed and recorded using GammaVision software.

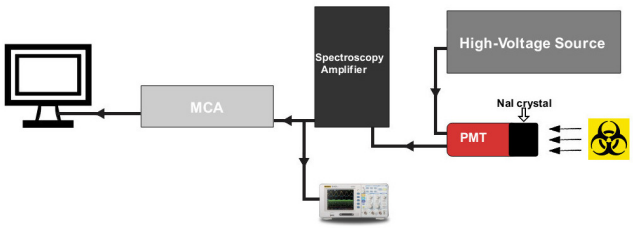

FIG. 1. Experimental setup for gamma ray spectroscopy. A NaI crystal detects gamma emissions from the radioactive source and re-emits them as visible photons. The photons travel to the photomultiplier tube (PMT), where they produce a signal that is amplified by the spectroscopic analyzer before reaching the multichannel analyzer (MCA), which sorts each pulse according its energy.

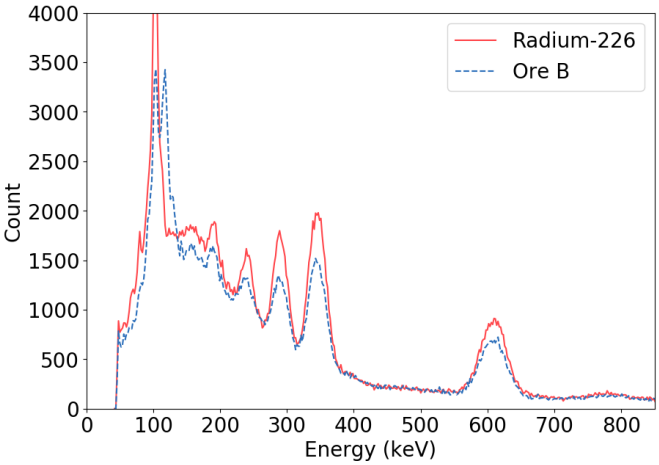

FIG. 2. A visual comparison of Ore B with ^{226}Ra suggests that they are the same radionuclide.

MEASUREMENTS

All measurements were performed in Lab 317 in the University of New Hampshire's DeMeritt Hall.

Gamma spectra were recorded on two separate occasions. The second data were necessary because the first data included an overly attenuated spectra that was inadequate for performing the lead attenuation measurement.

For data set 1, seven spectra were recorded: two of known radioactive sources (Cesium-137 and Radium-226), two of unidentified sources, one with a lead attenuator, and two with no source present (background).

For data set 1, each radioactive source was positioned 20±0.5 cm in front of the NaI detector "hot end." This distance was chosen to optimize the emission cross-section at the detector, permitting the NaI crystal to "see" the maximum number of decay events without exceeding the response time of the detector. The signals from the photomultiplier were amplified by a factor of 500. All spectra were recorded for 200 seconds (real time), except for the second background measurement, which ran for 300 seconds (real time).

An unidentified source labeled "Ore B" was measured, and a visual comparison to the Radium-226 spectrum revealed that it was very likely Radium-226 (Fig. 2). A measurement was also made with a different source, labeled "No. 3."

For data set 2, six spectra were recorded: Cesium-137 and Radium-226, one background, sample No. 3, and two Radium-226 with lead attenuator. Each source was placed 20±0.5 cm in front of the detector. The signals were amplified by a factor of 1000 and recorded for 180 seconds (live time). A different lead absorber (thicknesses 1.5±0.3 mm and 7.0±0.5 mm) was used for each of the lead attenuation measurements. For both measurements, the lead absorber was placed between the radioactive source and the detector, approximately 10 cm in front of the detector hot end.

Calibration—Prior to identifying sample No. 3 and measuring the mass attenuation coefficient of lead, we calibrated the spectra by mapping the photopeak energies of the two known sources to the channels of the MCA. Because our data were gathered on two separate occasions, it was necessary to perform separate calibrations for each data set. The calibration results for data set 1 are presented here, with results from data set 2 given in the Appendix.

We performed the calibration by first subtracting the recorded background spectrum from the Cesium-137 and Radium-226 spectra and fitting the local background to an exponential plus constant. We then fit the most prominent energy photopeaks to a Gaussian,

$$Ae^{\frac{-(x-X)^2}{2\sigma^2}}, \tag{1}$$

where X represents the MCA channel number of the photopeak max, σ is the width parameter, and A is the amplitude of the photopeak (Fig. 3).

The photopeak energies for Cesium-137 and Radium-226 were obtained from [8] and [9], and their errors were taken to be negligible. The resulting fit parameters, given in Table I, were used to determine a linear relationship between the gamma energies and the channels of the MCA (Fig. 4).

Errors on the linear fit parameters were calculated using standard methods from [10]. The equations are given in the Appendix.

Our results indicate an offset of 53±6 keV for our energy axis, with a resolution of 1.92±0.02 keV per channel, or a relative resolution of 6.0±0.3%, which we calculated using

$$\frac{1}{n}\sum_{i=1}^{n}\frac{2m\sigma_i}{E_i}\times 100, \tag{2}$$

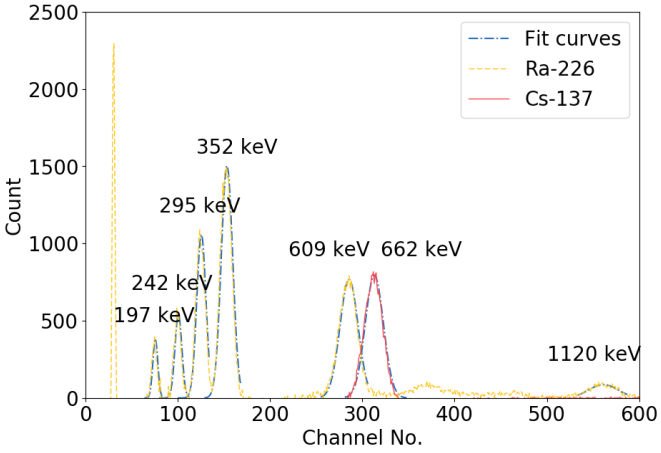

FIG. 3. The most prominent photopeaks of ^{137}Ce and ^{226}Ra were fitted to a Gaussian after removing global and local background noise from the spectra. The photopeak energies were obtained from tables of known decays.

TABLE I. Photopeak Fit Parameters.

Energy (keV)	ADC Channel No.
1120	560±16
661.64	310±10
609.312	290±10
351.932	153±6
295.224	126±5
241.997	101±4
187.1	76±3

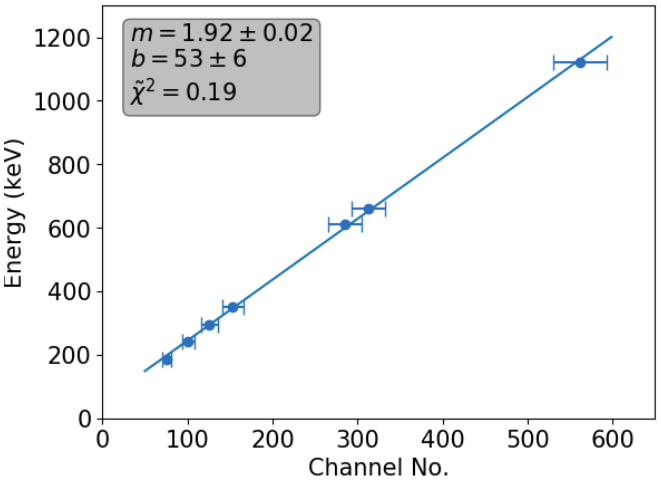

FIG. 4. A plot of known photopeak energies and MCA channel numbers, obtained from fitting the photopeaks to Gaussian curves, shows a strong linear relationship in the measured energy range.

where σ is the width parameter of the peak, E is the photopeak energy, m is the channel resolution, and n is the number of photopeaks measured.

RESULTS

Identity of unknown sample—Sample No. 3 was plotted on a calibrated energy axis and its photopeaks fitted to Gaussians. The energies, with one standard deviation errors, were found to be 560±20 keV and 1070±29 keV, as shown in Fig. 5.

To identify the source, we used the Nuclear Data Center at KAERI's "Table of Gamma Rays" [11] to narrow the search to radionuclides with prominent photopeaks that matched our results. Bismuth-207 was the only result that fit our search that contained no additional prominent photopeaks, which we would not have been able to account for in our data. Our data also show a large X-ray spike at approximately 75 keV, consistent with the decay spectrum of Bismuth-207.

Bismuth-207 undergoes three major gamma decays: 570 keV (97.74 I_γ), 1.064 MeV (74.5 I_γ), and 1.770 MeV(6.87 I_γ), where I_γ is the number of counts per 100 decays [12]. It's unclear whether the less-intense 1.770 MeV photopeak is present in our data. A longer acquisition time would likely help resolve this photopeak.

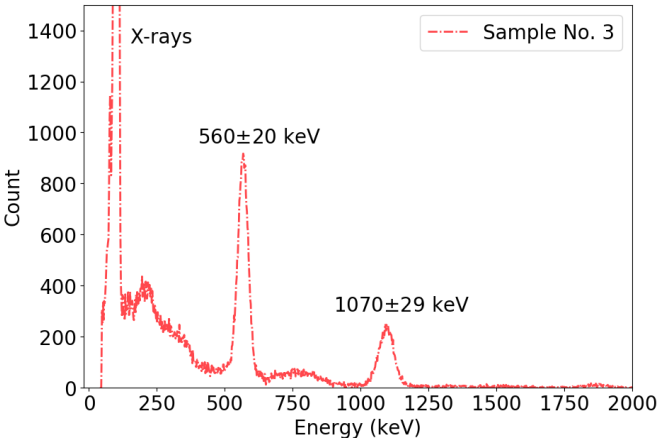

FIG. 5. Gamma spectrum of sample No. 3 with energy calibration: the two major photopeaks closely match the 570 keV and 1.064 MeV photopeaks of Bismuth-207.

Mass attenuation of lead at 609 keV—As mentioned in the Measurements section, it was necessary to obtain a second set of spectra to perform the lead attenuation measurements. The calibration results for data set 2 are given in the Appendix.

A background spectrum was subtracted from the three Radium-226 spectra, which were then fitted to a linear function to remove any remaining background from the 609 keV photopeaks. These photopeaks were then fitted to Gaussians, and the area under each curve was calculated, the results of which are shown in Figure 6. Errors on the counts were calculated using one standard deviation errors of the fit parameters, A and σ.

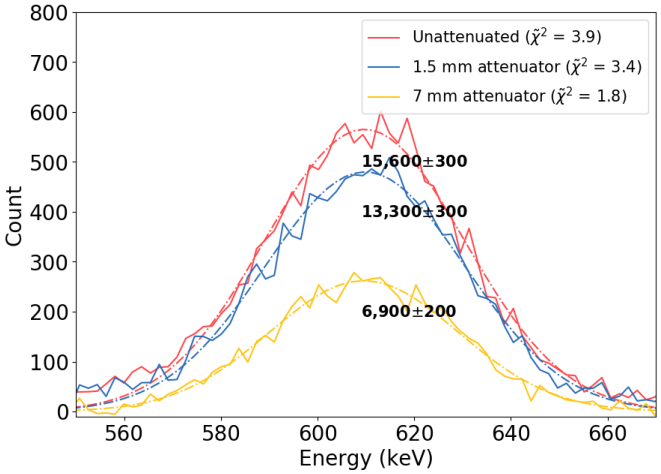

FIG. 6. Lead attenuation of the 609 keV photopeak of ^{226}Ra, showing the total number of counts under each curve.

We used these results to calculate the mass attenuation coefficient for lead, using

$$I(x) = I_0 e^{-\mu_\rho x \rho}, \tag{3}$$

where I and I_0 are the attenuated and unattenuated counts under the fit curves, respectively, x is the thickness of the absorber, ρ is the mass density of lead (11.35 g/cm^3), and μ_ρ is the mass attenuation coefficient.

Our results, summarized in Table II, yield 0.10±0.03 cm^2/g for the 1.5 mm absorber and 0.103±0.008 cm^2/g for the 7 mm absorber. To calculate the error in our results, we considered uncertainties in the counts under each curve, as well as in the thickness of the absorbers. The larger uncertainty on the 1.5 mm measurement can be largely accounted for by our having used an uneven absorber whose thickness could not be determined with greater precision.

TABLE II. Mass Attenuation of Lead.

Energy (keV)	μ_ρ (cm^2/g)
609 (1.5 mm absorber)	0.10±0.03
609 (7 mm absorber)	0.103±0.008
600 (from NIST)	0.1248

The result from the 1.5 mm absorber is consistent with the value of 0.1248 cm^2/g for 600 keV radiation, published by the National Institute of Standards and Measurements (NIST) [13]. The result from the 7 mm absorber is 11-23% smaller than the NIST value. Some of this discrepancy can be accounted for by the 9 keV energy difference between the NIST measurement and the 609 keV Radium peak. However, it is unlikely that this alone would account for the full discrepancy, suggesting that other experimental factors contributed. One possibility is that the cross-sectional area of the 7 mm absorber was insufficient to attenuate the incident gammas. Another possibility is that the placement of the 7 mm absorber relative to the source and detector affected the results. Additional experimentation would help eliminate some of these factors.

CONCLUSIONS AND REMARKS

The results of this experiment validate gamma spectroscopy using a NaI detector as a method for identifying and measuring radioactivity. However, measures could be taken to improve the precision of the results. For instance, lead shielding could be used to reduce the global background noise that was present in all gamma spectra. Longer data acquisition times would likely result in sharper photopeaks, which would

We wish to thank Professor Elena Long of the University of New Hampshire for her mentorship throughout this project and her feedback on an earlier draft of this paper. We also recognize Luke Jameson for his insights in data analysis and Kyle Morman and Lars Luxem for their help in setting up the experiment.

APPENDIX

Energy calibration of data set 2—

Error calculations for energy calibration—Errors on the linear fit parameters used in the energy calibrations were calculated using the following relations from [10]:

$$\sigma_b = \sigma_y \sqrt{\frac{\sum_{i=1}^{N} x_i^2}{\Delta}} \tag{4}$$

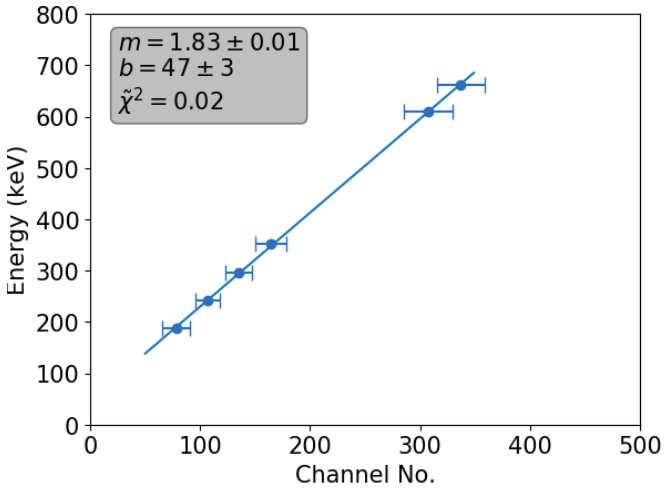

FIG. 7. Energy calibration results for data set 2. The relative resolution of the detector was 8.1 ± 0.3%.

$$\sigma_m = \sigma_y \sqrt{\frac{N}{\Delta}} \tag{5}$$

Here N is the number of photopeaks fitted, x is the MCA channel location of each photopeak, σ_y is the uncertainty in the y-values, obtained from

$$\sigma_y = \sqrt{\frac{1}{N-2}\sum_{i=1}^{N}(y_i - b - mx_i)^2}, \tag{6}$$

and Δ is found from

$$\Delta = N\sum_{i=1}^{N} x_i^2 - (\sum_{i=1}^{N} x_i)^2. \tag{7}$$

* kjm1042@wildcats.unh.edu

[1] Health Physics Society, Background Radiation: Fact Sheet (2018). [Available at https://hps.org/documents/background_radiation_factsheet.pdf]

[2] United States Nuclear Regulatory Commission, Backgrounder on Biological Effects of Radiation (2018). [Available at https://www.nrc.gov/reading-rm/doc-collections/fact-sheets/bio-effects-radiation.html]

[3] T. Adagunodo, A. George, I. Ojoawo, K. Ojesanmi, R. Ravisankar, Radioactivity and radiological hazards from a kaolin mining field in Ifonyintedo, Nigeria. MethodsX, 5, 362-374 (2018).

[4] H. Taskin, M. Karavus, P. Ay, A. Topuzoglu, S. Hidiroglu, G. Karahan, Radionuclide concentrations in soil and lifetime cancer risk due to gamma radioactivity in Kirklareli, Turkey. Journal of Environmental Radioactivity, 100(1), 49-53 (2009).

[5] D. Griffiths, Introduction to Elementary Particles (2008).

[6] E. Long, PHYS 705/805 Nuclear Physics Workshop Parts I/II. (Presentation). Durham, NH: Univ. of New Hampshire (2018).

[7] W.R. Leo, Techniques for Nuclear and Particle Physics Experiments: A How-to Approach (1994).

[8] Radionuclide Data Sheet: Cesium 137. Spectrum Techniques, LLC. [The data are available at http://www.spectrumtechniques.com/wp-content/uploads/2016/12/Cesium-137-Information-Sheet.pdf]

[9] Gamma-Ray Energies and Intensities, ^{226}Radium. Radiochemistry Society. [The data are available at www.radiochemistry.org/periodictable/gamma_spectra/pdf/ra226.pdf]

[10] R.J. Taylor, An Introduction to Error Analysis: The Study of Uncertainties in Physical Measurements (1997).

[11] Nuclear Data Center at KAERI, "Table of Gamma Rays," [The data are available at http://atom.kaeri.re.kr/]

[12] Gamma-Ray Energies and Intensities, ^{207}Bismuth. Radiochemistry Society. [The data are available at https://www.radiochemistry.org/periodictable/gamma_spectra/pdf/bi207.pdf]

[13] J.H. Hubbell, S.M. Seltzer, Tables of X-Ray Mass Attenuation Coefficients and Mass Energy-Absorption Coefficients 1 keV to 20 MeV for Elements Z=1 to 92 and 48 Additional Substances of Dosimetric Interest. 72. NIST (1995).